The α/β-hydrolase domain-containing 4- and 5-related phospholipase Pummelig controls energy storage in *Drosophila*

Philip Hehlert,[1,2,*] Vinzenz Hofferek,[†] Christoph Heier,[3,§] Thomas O. Eichmann,[§] Dietmar Riedel,[**] Jonathan Rosenberg,[4,*] Anna Takaćs,[*] Harald M. Nagy,[§] Monika Oberer,[§,††] Robert Zimmermann,[§,††] and Ronald P. Kühnlein[1,*,§,††]

Research Group Molecular Physiology* and Department of Structural Dynamics, Electron Microscopy,** Max-Planck-Institut für Biophysikalische Chemie, Göttingen, Germany; Max-Planck-Institut für Molekulare Pflanzenphysiologie,[†] Potsdam, Germany; Institute of Molecular Biosciences,[§] University of Graz, Graz, Austria; and BioTechMed-Graz,[††] Graz, Austria

ORCID IDs: 0000-0003-3794-3267 (P.H.); 0000-0003-1448-4117 (R.P.K.)

Abstract Triglycerides (TGs) are the main energy storage form that accommodates changing organismal energy demands. In *Drosophila melanogaster*, the TG lipase Brummer is centrally important for body fat mobilization. Its gene *brummer* (*bmm*) encodes the ortholog of mammalian adipose TG lipase, which becomes activated by α/β-hydrolase domain-containing 5 (ABHD5/CGI-58), one member of the paralogous gene pair, α/β-hydrolase domain-containing 4 (*ABHD4*) and *ABHD5*. In *Drosophila*, the *pummelig* (*puml*) gene encodes the single sequence-related protein to mammalian ABHD4/ABHD5 with unknown function. We generated *puml* deletion mutant flies, that were short-lived as a result of lipid metabolism changes, stored excess body fat at the expense of glycogen, and exhibited ectopic fat storage with altered TG FA profile in the fly kidneys, called Malpighian tubules. TG accumulation in *puml* mutants was not associated with increased food intake but with elevated lipogenesis; starvation-induced lipid mobilization remained functional. Despite its structural similarity to mammalian ABHD5, Puml did not stimulate TG lipase activity of Bmm in vitro. Rather, Puml acted as a phospholipase that localized on lipid droplets, mitochondria, and peroxisomes. Together, these results show that the ABHD4/5 family member Puml is a versatile phospholipase that regulates *Drosophila* body fat storage and energy metabolism.—Hehlert, P., V. Hofferek, C. Heier, T. O. Eichmann, D. Riedel, J. Rosenberg, A. Takaćs, H. M. Nagy, M. Oberer, R. Zimmermann, and R. P. Kühnlein. **The α/β-hydrolase domain-containing 4- and 5-related phospholipase Pummelig controls energy storage in *Drosophila*. *J. Lipid Res.* 2019.** 60: **1365–1378.**

Supplementary key words lipid and lipoprotein metabolism • obesity • storage diseases • phospholipids/metabolism • Malpighian tubules • adipose triglyceride lipase • Brummer (*Drosophila melanogaster* adipose triglyceride lipase)

Organismal energy homeostasis is continuously challenged by fluctuating environmental and internal conditions, which require a fast and precisely controlled adaption to energy needs. To maintain this homeostasis, organisms as different as yeast, plants, nematodes, flies, mice, and humans accumulate energy stores during periods of food supply. Whenever energy expenditure exceeds energy intake, these energy stores become mobilized and catabolized to ensure permanent energy balance. Lipids, in particular triglycerides (TGs), are the calorically most important energy depots in eukaryotic organisms. Besides their pivotal function as metabolic fuel, i.e., as a source of FAs for β-oxidation,

Abbreviations: ABHD4, α/β-hydrolase domain-containing 4; ABHD5, α/β-hydrolase domain-containing 5; ATGL, adipose triglyceride lipase; bmm, brummer; CGI-58, comparative gene identification-58; CL, cardiolipin; Em, emission; Ex, excitation; LD, lipid droplet; MT, Malpighian tubule; NAE, *N*-acylethanolamine; NAPE, *N*-acylphosphatidylethanolamine; PA, phosphatidic acid; PG, phosphatidylglycerol; puml, pummelig (CG1882); TG, triglyceride.

[1] To whom correspondence should be addressed.
e-mail: ronald.kuehnlein@uni-graz.at (R.P.K); philip.hehlert@uni-goettingen.de (P.H.)

[2] Present address of P. Hehlert: Georg-August-University Göttingen, Johann-Friedrich-Blumenbach Institute for Zoology and Anthropology, Abteilung Zelluläre Neurobiologie, Schwann-Schleiden Forschungszentrum, Julia-Lermontowa-Weg 3, D-37077 Göttingen, Germany.

[3] Present address of C. Heier: University of Graz, Institute of Molecular Biosciences, Humboldtstrasse 50, A-8010 Graz, Austria.

[4] Present address of J. Rosenberg: Georg-August-University Göttingen, Department for General Microbiology, Griesebachstr. 8, D-37077 Göttingen, Germany.

[S] The online version of this article (available at http://www.jlr.org) contains a supplement.

This study was supported by the Max-Planck-Gesellschaft (D.R., R.P.K), Austrian Science Fund (FWF) Project P22170 (M.O.), SFB LIPOTOX (F30; M.O.), and doctoral school "DK Molecular Enzymology" (W901; M.O., R.Z.). The authors declare that they have no conflicts of interest with the contents of this article.

Manuscript received 28 January 2019 and in revised form 3 June 2019.

Published, JLR Papers in Press, June 4, 2019
DOI https://doi.org/10.1194/jlr.M092817

intermediates of TG catabolism provide building blocks for a variety of lipids with structural and signaling function. Due to the cross-talk within the lipid metabolism network, a variety of dysfunctions can manifest in excessive body fat accumulation, with human obesity being the most prominent example. However, neutral lipid over-storage is not restricted to tissues dedicated to fat storage, such as mammalian adipose tissue or the so-called fat body of insects. Rather, ectopic lipid storage as a hallmark of uncontrolled local or global lipid homeostasis is widespread in multicellular eukaryotes, as in *Drosophila* brain glial cells (1) or *Arabidopsis* leaves (2). Importantly, the physiological consequences of ectopic fat accumulation are only poorly understood.

The universal packaging of storage lipids in unique organelles called lipid droplets (LDs) is a common motive of fat storage in many cell types. The remarkable structural and regulatory similarities of LDs in a wide range of organisms point to evolutionary ancestry of the network in control of the metabolic dynamics of LDs. Indeed, comparative physiological and genetic studies in a variety of organisms revealed that central regulators acting on LDs are evolutionarily conserved. Examples in the fly are the LD-associated perilipins [*Dm*Plins (3–6)] or the key TG biosynthesis gene *midway*, which encodes the *Drosophila* diacylglycerol *O*-acyltransferase 1 [*Dm*Dgat1 (4, 7, 8)]. Central to TG lipolysis is the *brummer* (*bmm*, *DmATGL*) gene (9), which encodes the ortholog of the mammalian adipose TG lipase [ATGL (10, 11)].

Comparative gene identification-58 (CGI-58), also known as α/β-hydrolase domain-containing 5 (ABHD5) (12) is one member of the paralogous protein pair, α/β-hydrolase domain-containing 4 (ABHD4) and ABHD5, and acts as coactivator of mammalian ATGL. ABHD5/CGI-58 physically interacts with perilipin 1 on the LD surface (13–16). Upon lipolytic stimulation, ABHD5/CGI-58 dissociates from perilipin 1 and stimulates TG lipase activity of ATGL by a so far unknown mechanism (13). A knockout of mammalian *ATGL* (17) or *ABHD5/CGI-58* (18) causes neutral lipid storage disease in mice and humans. However, knockout mutations in these genes result in different phenotypes (18) [recently reviewed in (19, 20)]. In contrast to *ATGL* knockout mutants, mice lacking *ABHD5/CGI-58* exhibit ichthyosis, skin permeability defects, more severe hepatic steatosis, and altered acyl-ceramide production (21). These data strongly support *ATGL*-independent functions for *ABHD5/CGI-58*. It is likely that mammalian ABHD5/CGI-58 cooperates with other enzymes to execute ATGL-independent functions, as the protein is catalytically inactive due to replacement of the active serine within the conserved GxSxG lipase motif by an asparagine (**Fig. 1A**) (14, 22, 23). Recently, it has been shown that ABHD5 interacts with patatin-like phospholipase domain-containing 1 (PNPLA1), recruiting this enzyme to LDs and modulating its acyl-ceramide synthesis activity (24).

In contrast to ABHD5/CGI-58, the paralogous ABHD4 is an active lipid hydrolase, which is involved in anoikis resistance (25) and endocannabinoid biosynthesis (26).

The characteristics of the ABHD4 and ABHD5/CGI-58 protein pair are consistent with the hypothesis that they evolved from an ancestral enzyme, which underwent gene duplication and functional diversification in the mammalian lineage (27).

ABHD4/5-related genes are found in diverse species beyond mammals. In all cases studied, the lack of ABHD4/5 consistently leads to altered neutral and/or phospholipid metabolism as demonstrated in mice (28–31), in the thale cress *Arabidopsis thaliana* (2), in the yeast *Saccharomyces cerevisiae* (32), and in the nematode *Caenorhabditis elegans* (33, 34). Notably, however, *C. elegans* encodes multiple ABHD4/5-related proteins, two of which, the ABHD4-relative *Ce*Lid-1 (33) and the ABHD5/CGI-58-relative *Ce*Abhd5.2 (34), interact with *Ce*ATGL-1, determine its localization to LDs, and thereby control lipolysis comparable to their mammalian homologs.

This study presents the functional characterization of CG1882, which we renamed Pummelig (Puml; colloquial German for chubby) in accordance with the mutant phenotype (see below). Pummelig is the single *Drosophila melanogaster* α/β-hydrolase domain protein, which is sequence-related to the mammalian paralogs, ABHD4 and ABHD5/CGI-58. We showed that *pummelig* deletion mutants (*puml*^{1}) suffered from defects in overall physical fitness and accumulated extra body fat. These obese flies were still capable of mobilizing storage lipids and exhibited increased lipogenesis. Additionally, abnormal lipid storage could be detected in fly kidneys, called Malpighian tubules (MTs), and the FA profile of these ectopically stored TGs was altered in flies lacking *puml* function. In contrast to mammalian ABHD5, Puml did not stimulate TG lipase activity of Brummer (*Dm*ATGL) in vitro. Besides exhibiting no autonomous TG lipase activity, Puml actually is a functional phospholipase. Tagged Pummelig localized to various intracellular compartments in vivo, i.e., LDs, mitochondria, and peroxisomes.

MATERIALS AND METHODS

Fly husbandry and stocks

Flies were propagated on a complex medium as described (35). For further details, see the supplemental Experimental Procedures. The fly stocks used in this study are listed in supplemental Table S1 in the supplemental Experimental Procedures.

A *puml*^{1} deletion mutant was generated by a conventional P-element mobilization scheme using the P{SUPor-P}CG1882[KG09852] (36) fly line, that carried a P-element insertion in the *puml* 5′UTR (Fig. 1B). Subsequent molecular characterization by sequencing the relevant part of the genome revealed an imprecise excision with 12 bp residual P-element sequence remaining between the deletion breakpoints and *puml* gene locus being devoid of coding DNA sequence from position 188-2369 relative to the transcription start of *puml*-RA cDNA. For appropriate and biologically comparable controls, the obtained *puml*^{1} mutant allele was backcrossed several generations into w^{1118} fly stock (referred to as control stock) to get genetically matched flies. For other transgenic fly stocks, additional information can be found in the supplemental Experimental Procedures. Transgenic fly stocks were obtained from the Vienna Drosophila Resource Center (VDRC, www.vdrc.at). Stocks obtained from the Bloomington Drosophila Stock Center (NIH P40OD018537) were used in this study.

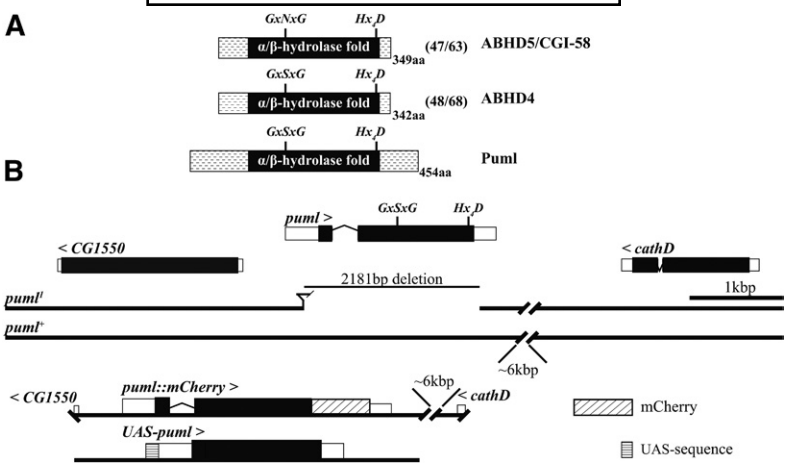

Fig. 1. Scheme of the ABHD4/5-related Pummelig protein and of the *pummelig* gene locus. A: Comparison (percent identity/percent similarity) of the primary protein structure of Puml to the human paralogs ABHD4 and ABHD5/CGI-58. Note: Consistent with ABHD4 but unlike ABHD5/CGI-58, Puml carries an intact GxSxG lipase nucleophile motif, whereas all three proteins share a Hx_4D motif. Black boxes indicate the extent of the α/β hydrolase fold domain. B: Extended genomic region of *puml* (formerly called *CG1882*) flanked by *CG1550* and *cathD*. Molecular structure of the *puml* deletion mutant (*puml*^{l}) and of the genomic and cDNA-based *puml* rescue constructs. The genomic rescue transgene covers the *puml* gene region from the 5′UTR of *CG1550* to the 3′UTR of *cathD* and contains a C-terminal mCherry-tag. The cDNA-based transgene contains the *puml-RA* isoform under the control of the UAS sequence for conditional gene expression. Note that only the A isoforms, RA and PA, for transcript and proteins, respectively, are shown for the corresponding genes. For simplicity, Puml is used for Puml-PA in the text. Black boxes indicate coding regions, and open boxes indicate untranslated regions of the transcription units. The > or < indicate the direction of transcription of the respective genes.

Physiological assays

Lipid analysis. Fly body fat content and total body neutral lipids (TGs, DGs) were quantified by a coupled colorimetric assay (37) and by thin-layer chromatography as described (35). For further details, see the supplemental Experimental Procedures.

Glycogen analysis. Stored glycogen of flies was quantified as described (35). For further details, see the supplemental Experimental Procedures.

Food intake. Food intake of ad libitum-fed flies was determined as described (38). For further details, see the supplemental Experimental Procedures.

Weight measurements. Empty 1.5 ml vials were labeled and weighed. Thirty flies per replicate were collected and anesthetized with CO_2. After weighing (wet weight) flies were snap-frozen in liquid nitrogen and dried overnight (65°C, 5% humidity). Then flies were weighed again (dry weight). The fly water content was calculated by subtracting dry weight from wet weight.

Starvation, desiccation, and locomotor activity assay. Six-day-old male flies were briefly anesthetized with CO_2, and individual flies were quickly transferred to 5 mm diameter glass tubes of the *Drosophila* activity monitor 2 (DAM2) system (TriKinetics Inc., Waltham, MA). For the starvation assay, water was supplied in the form of 2% agarose at one end of the tube. For the desiccation assay, empty tubes were used. Genotypes were distributed randomly over the monitors and kept under standard conditions. Cumulative light-beam passes (activity) were read out every 5 min. Dead flies were scored using the last point of measured activity. Survival analysis was performed in OriginPro 9.1 using Kaplan-Meier analysis and a log rank test.

Locomotor activity was calculated from the total accumulated activity per fly measured in the DAM2 system during the first 24 h of starvation.

Energy expenditure. The metabolic rate of 6-day-old flies was estimated by the manometric measurement of CO_2 production as described in (39). For further details, see the supplemental Experimental Procedures.

Lipogenesis assay. Lipogenesis in adult flies was traced by incorporation of D-[^{14}C(U)]glucose into neutral lipids as described in (40). For details, see the supplemental Experimental Procedures.

Enzymatic assays. TG hydrolase activity was measured as described in (41). For further details, see the supplemental Experimental Procedures. The substrate screen on Puml was performed as described in (42). Tested substrates and their suppliers are listed in supplemental Table S3. Substrate saturation, pH, protein, and time dependence of the hydrolase activity were measured as essentially described in (43). For details on cloning and protein expression, see the supplemental Experimental Procedures.

Imaging

Images from adult fat body tissue were obtained as described in (38). To acquire images from MTs, 6-day-old male flies were dissected in ice-cold 1× PBS. Flies were grabbed with forceps at the thorax and the anal plate. Then both forceps were gently pulled apart. Along with the intestine, the MTs were pulled out from the abdomen. The MTs (together with the intestine) were then embedded in 1× PBS containing Bodipy493/503 (38 μM; Invitrogen, D3922) or LipidTOX DeepRed (2×; Invitrogen, H34477) for LD staining, DAPI (3.6 μM; Invitrogen, D1306) for nuclei staining, and CellMask™ Deep Red (5 μg/ml; Invitrogen, C10046) for plasma membrane staining. Images were acquired with a Zeiss

ASBMB JOURNAL OF LIPID RESEARCH

LSM-780 microscope (at 20°C) in 16-bit mode using a C-Apochromat 40×/1.20 W Korr FCS M27 objective and the Zeiss ZEN software. For fluorescence detection, the following settings were used: DAPI [excitation (Ex): 405 nm; emission (Em): 410–468 nm]; Bodipy493/503 (Ex: 488 nm; Em: 490–534 nm); and CellMask (Ex: 561 nm; Em: 585–747 nm). For the detection of fluorescent proteins, the following settings were used: eGFP (Ex: 488 nm; Em: 490–540 nm); ECFP (Ex: 405 nm; Em: 450–540 nm); and mCherry (Ex: 561 nm; Em: 570–712 nm). Mitochondria were stained by Mitotracker Orange CMTMRos (75 nM; Invitrogen, M7510; Ex: 561 nm; Em: 570–590 nm). Images were subsequently processed in Image J v1.49m and Adobe Illustrator CS6.

Lipid staining with Oil Red O. LDs were stained with Oil Red O as described in (38). For further details, see the supplemental Experimental Procedures.

Electron microscopy. Ultrastructural analyses of MTs were performed as described for fat body tissue (38). For further details, see the supplemental Experimental Procedures.

LD size quantification. An improved protocol for LD size quantification based on (35) was used. Various optimizations were introduced to detect especially small and weakly stained LDs and balance out inhomogeneous LD signals and, therefore, get a more reliable detection of LDs by the particle analyzer plug-in of ImageJ v1.49m. For detailed information see the supplemental Experimental Procedures.

Lipidomics (dataset 1)

Five replicates of 10 MT pairs (per genotype) were obtained from 6-day-old male animals. Fly dissection was performed in ice-cold Ringer solution. Samples were collected in 1.5 ml SAFE-lock Eppendorf tubes (T2795-1000EA) and buffer was removed as much as possible. Then samples were snap-frozen in liquid nitrogen. Lipids were extracted from tissue by a modified protocol from (44). In detail, 1 ml of precooled (−20°C) extraction solvent [methanol:methyl tertiary butyl-ether (1:3, v/v)] was added to the tissue and well mixed. The solvent-homogenate solution was incubated for 30 min (4°C) under constant shaking, followed by a 10 min incubation in an ultrasonication bath filled with an ice-water mix. For phase separation, 650 µl of water:methanol (3:1, v/v) were added, mixed, and centrifuged for 5 min at 4°C at 21,000 *g* in a tabletop Eppendorf centrifuge. Six hundred microliters of the resulting upper lipid-containing phase were transferred to a new 1.5 ml Eppendorf tube, dried in a speed-vac concentrator, and stored at −80°C. As control for the extraction and for the analysis, PC (17:0/17:0) (Avanti Polar Lipids, 850360C) was added as an internal standard at a concentration of 0.1 µg/ml.

Liquid chromatography was performed following the protocol of Hummel et al. (44). Dried lipid extracts were resuspended in 300 µl 7:3 (v/v) acetonitrile:2-propanol. For separation of lipids, a Waters Acquity UPLC system with a Waters C8 reversed-phase column (100 × 2.1 mm, 1.7 µm particle size) was used. Flow rate was set to 400 µl/min, column temperature was set to 60°C, and samples were kept cooled at 10°C in the autosampler. Of this sample, 5 µl were loaded onto the C8 column. For elution, a gradient of two mobile phases (A and B) was used. Phase A was water and phase B consisted of acetonitrile:isopropanol (7:3, v/v); both phases contained 1% (v/v) 1 M ammonium acetate and 0.1% (v/v) acetic acid. The elution gradient was 1 min 45% A, in 4 min from 45% A to 25% A, in 12 min from 25% A to 11% A, in 15 min from 11% A to 0% A (=100% B), for 4.5 min 100% B, and back to 45% A, equilibrating for 4.5 min before the next elution, giving the total of 24 min for one run.

Mass spectrometric analysis was performed using an LTQ-Orbitrap XL instrument using the following parameters: mass range, normal; resolution, 60,000; scan type, full; data type, profile; scan range, *m/z* 150–1,500. We used a heated ES source with the following settings: heater temperature, 350°C; gas flow rates (sheath gas, 20; aux gas, 16; sweep gas, 0). Spray voltage was set to 3.2 kV in negative mode and 3.5 kV in positive mode. Capillary was set to ±35 V and heated to 275°C, and tube lens to ±110 V for (+) positive and (−) negative mode.

RESULTS

Pummelig controls organismal energy stores

In order to characterize the *puml* gene function in vivo, a deletion mutant ($puml^1$) was generated, covering the complete *puml* coding region (Fig. 1B). Homozygous $puml^1$ flies were viable and fertile. However, compared with control flies, $puml^1$ flies were significantly short-lived (**Fig. 2A**). Additionally, startle-induced climbing activity in $puml^1$ flies was significantly lower compared with controls (Fig. 2B) and $puml^1$ flies weighed less due to reduced body water content (Fig. 2C). On the other hand, critical physiological parameters such as the respiratory rate under fed and starved conditions (Fig. 2D), spontaneous locomotor activity under starvation (Fig. 2E), and food intake (Fig. 2F) were normal in $puml^1$ flies compared with controls.

Collectively, these data demonstrate that *puml* is not an essential gene but controls selective physical fitness parameters in flies.

Proper energy homeostasis is critical for physical fitness, and therefore we analyzed energy storage in $puml^1$ flies. $puml^1$ flies accumulated less glycogen compared with control flies, which could be properly mobilized during starvation (**Fig. 3A**). Consistent with glycogen being an important metabolic water reservoir and with the finding that $puml^1$ flies had overall lower body water content (Fig. 2C), flies lacking Puml were desiccation sensitive (Fig. 3B).

Due to the high similarity of Pummelig to mammalian ABHD5, we investigated whether $puml^1$ flies also had altered lipid metabolism. Indeed, $puml^1$ flies of both sexes accumulated excess body fat from early adult stages onwards (Fig. 3C; supplemental Figs. S2, S3A, B) similar to bmm^1 (DmATGL$^{-/-}$) mutant flies (9). Organ-specific *puml* function in the fly fat storage tissue is critical because the obese phenotype of the deletion mutant ($puml^1$) could be phenocopied by a tissue-specific *puml* gene knockdown exclusively in the fat body (Fig. 3C). In contrast to *bmm* (9), in vivo overexpression (gain-of-function) of *puml* in the fat body had no significant effect on body fat stores (Fig. 3C). As the extra body fat is metabolically accessible, obese $puml^1$ flies were more starvation resistant than control flies (Fig. 3D). Notably, compared with controls, significantly more neutral lipids were mobilized in $puml^1$ flies during the first 24 h of starvation (Fig. 3E). Whereas $puml^1$ flies mobilized 18.6 ± 2.1 µg TG, control flies utilized 14.3 ± 0.4 µg storage lipids (one-way ANOVA $F_{1,24}$ = 61.11, P = 6.36E-8). This might be a consequence of low glycogen stores (Fig. 3A), as carbohydrates represent the preferred energy

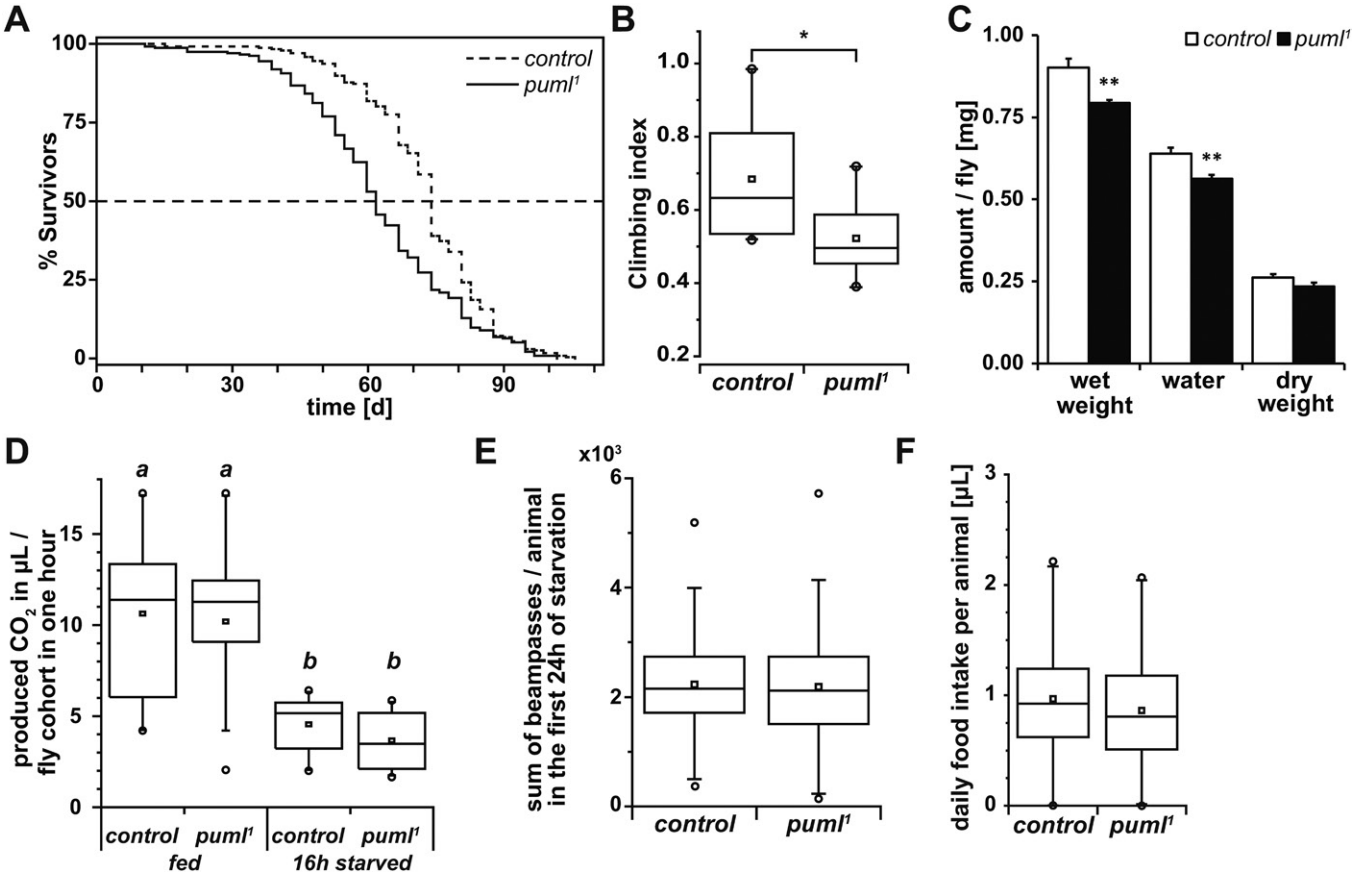

Fig. 2. Reduced lifespan and physiological fitness phenotypes of *pummelig* mutant flies. A: Decreased median lifespan of *puml*^{1} flies compared with genetically matched controls (log rank-*P* test; $P = 3{,}4726E\text{-}8$; n = 240 animals per genotype). B: Decreased startle-induced climbing activity in *puml*^{1} flies compared with controls (Mann-Whitney test, $*P < 0.05$). C: Reduced wet body weight and body water content of *puml*^{1} flies compared with control flies. D: Metabolic rate reduction in starved *puml*^{1} and control flies (16 h starved, 8 h after zeitgeber) compared with fed flies of the same genotypes (two-way ANOVA $F_{1,93} = 49.06$, $P = 4.16E\text{-}10$), but no metabolic rate difference between *puml*^{1} flies and controls under fed or starved conditions (two-way ANOVA $F_{1,93} = 0.53$, $P = 0.46$). Box plot represents the CO_2 (microliters) produced per hour and per fly cohort (three male flies); n > 20 for each genotype and condition. E: No difference in spontaneous locomotor activity (expressed as number of beam passes) during the first 24 h of starvation between *puml*^{1} mutant flies and controls (Mann-Whitney test; n = 63 for each genotype). F: No difference in food intake between *puml*^{1} mutant flies and controls (one-way ANOVA, $F_{(2,407)} = 1.92$, $P = 0.14$). Box plot of the daily food consumption (on 5% yeast extract + 5% sucrose) of the tested genotypes (followed from 6 days after enclosure for 6 days); n ⩾ 136 for each genotype. D–F: Box plot center lines show the median, box limits indicate the 25th and 75th percentiles as determined by OriginPro software; whiskers extend 1.5 times the interquartile range from the 25th and 75th percentiles.

source during early starvation. Interestingly, in spite of its increase during early fasting, the starvation-induced body fat mobilization was incomplete in *puml*^{1} flies (Fig. 3E), thus we cannot exclude an impairment of TG catabolism in *puml*^{1} flies.

As shown above, flies lacking *puml* function had normal food intake and reduced glycogen but increased fat storage under ad libitum feeding. Therefore, we hypothesized that in *puml*^{1} flies, dietary sugars might have a divergent channelling into the various energy stores compared with control flies. To address this question, we monitored in vivo lipogenesis in a pulse-chase experiment using radioactively labeled glucose. Pulse-feeding *puml*^{1} flies with food spiked with D-[^{14}C(U)]glucose for 24 h resulted in a significantly higher tracer incorporation into neutral lipids compared with controls (Fig. 3F), suggesting an increased lipogenesis rate. The difference between *puml*^{1} and control flies was even more pronounced after a 60 h chasing period on tracer-free food (Fig. 3F), indicating a slower turnover rate for storage lipids in *puml*^{1} flies. Consistent with increased lipogenesis in *puml*^{1} flies, the mRNA expression of the lipoanabolic genes, *FASN1* and acetyl-CoA carboxylase (*ACC*) (but not of *midway/DmDgat1*), were slightly increased compared with controls (Fig. 3G), notwithstanding that the encoded enzymes are subjected to functionally important posttranscriptional regulation, which was not addressed in this study.

Collectively, the organismal phenotypes of *puml*^{1} flies support a complex function of the *puml* gene in lipid metabolism and nutrient channelling to body energy stores.

pummelig mutant flies store ectopic LDs in the MTs

puml gene expression is not restricted to the fat body, the main energy storage tissue in fruit flies, but is widely expressed in adult *Drosophila*, including the fly kidneys, called MTs (45, 46). In contrast to MTs of adult control flies, which had very few LDs (**Fig. 4A–C**), *puml*^{1} flies showed

ASBMB JOURNAL OF LIPID RESEARCH

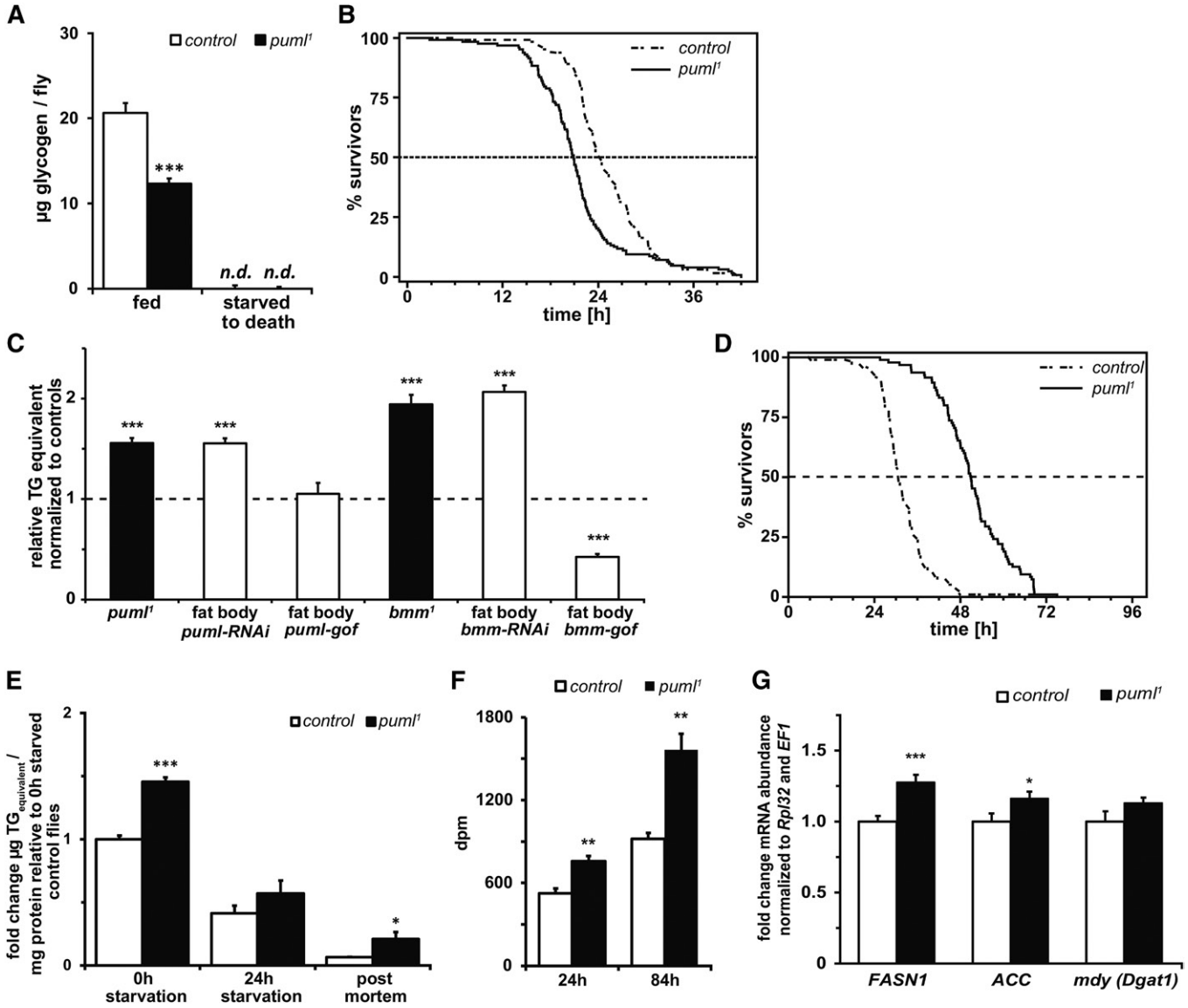

Fig. 3. *pummelig* loss-of-function selectively effects fly physical fitness and causes impaired lipid metabolism. A: Reduced glycogen stores in *puml*^{1} flies compared with control flies. Note that starvation-induced glycogen mobilization is complete in both genotypes. B: Desiccation sensitivity of *puml*^{1} flies is compared with control flies (log rank-*P* test; $P < 0.001$; n = 100 flies per genotype). C: Increased body fat in *puml*^{1} flies and in *bmm*^{1} deletion mutant flies and flies subjected to *puml* (*puml*-RNAi) or *bmm* (*bmm*-RNAi) gene knockdown targeted exclusively to the fat body. Fat body-targeted gene overexpression of *bmm* (*bmm-gof*) but not of *puml* (*puml-gof*) reduces fly body fat stores. D: Starvation resistance of obese *puml*^{1} mutant flies compared with controls (log rank-*P* test; $P < 0.001$; n = 100 flies per genotype). E: Functional but impaired starvation-induced body fat mobilization of *puml*^{1} flies compared with controls. Note the enhanced lipid reduction after the first 24 h under starvation and residual body fat post starvation of *puml*^{1} flies compared with control flies. F: Increased lipogenesis and reduced neutral lipid turnover in *puml*^{1} flies compared with controls. Shown is ^{14}C-labeled glucose in vivo incorporation into neutral lipids in *puml*^{1} flies compared with control flies after food-supplied 24 h pulse labeling followed by a 60 h chase on unlabeled food (84 h). G: Increased mRNA expression of lipogenic genes *FASN1* and acetyl-CoA carboxylase (*ACC*), but not of *mdy/Dgat1*, in *puml*^{1} flies compared with control flies. A, C, E–G: Shown are means ± SEM; Mann-Whitney test, ***$P < 0.001$, **$P < 0.01$, *$P < 0.05$, *n.d.*, not detectable.

strong lipid accumulation in this tissue (Fig. 4D–F). Lipidomic profiling of TGs in MTs revealed an increase of many TG species in *puml*^{1} flies compared with controls (Fig. 4G). Ubiquitous (Fig. 4I) or MT-specific (Fig. 4J) but not fat body-specific (Fig. 4K) *puml* expression rescued LD overstorage in MTs of *puml*^{1} flies (Fig. 4H). This demonstrates that ectopic LD accumulation in *puml*^{1} flies is due to the tissue-autonomous lack of Puml function in MTs. Consistent with this tissue-autonomous function and the limited lipid storage capacity of the fly kidney, MT-specific *puml* expression caused only a moderate reduction of the total body fat content of *puml*^{1} flies (Fig. 4L). In contrast, ubiquitous or fat body-specific *puml* expression reverted the obesity phenotype of the mutants to control levels (Fig. 4L).

MTs serve various functions in *Drosophila*, with osmoregulation being the most prominent. Because *puml*^{1} flies store less body water, we hypothesized that LD accumulation impairs the function of MTs in water balance. To address their osmoregulatory capacity, we monitored the survival of *puml*^{1} flies under salt stress. Control and *puml*^{1}

flies on a salty diet (food supplemented with 4% NaCl) outlived food-deprived flies but both comparably deceased within a week (Fig. 4M), suggesting that lipid accumulation in the MTs in *puml*^{1} flies has no major negative impact on osmoregulation.

Remarkably, lack of Puml function in MTs not only increased LD abundance but also altered the size distribution of the LD population. Compared with MT LDs of control flies, the droplets of *puml*^{1} flies showed a smaller average diameter and a more uniform size distribution (Fig. 4N), suggesting a role of Puml in the modeling of the LD structure.

Pummelig does not stimulate Brummer/DmATGL TG hydrolase activity in vitro

A key role of the mammalian Puml ortholog, ABHD5/CGI-58, is the activation of ATGL (12). In support of a putative ABHD5-like function of Puml, all currently known amino acids critical for the ABHD5/CGI-58 interaction with ATGL are sequence conserved in *Drosophila* Puml (Fig. 1A, supplemental Fig. S1). Therefore, we tested to determine whether Puml acts as a part of a Puml+Bmm lipid mobilization complex comparable to ABHD5/CGI-58+ATGL in mammals. To this aim, we recombinantly expressed Puml, Bmm, *Mm*ABHD5/CGI-58, and *Mm*ATGL, and determined TG hydrolase activity of *Mm*ATGL/Bmm in the absence or presence of Puml/*Mm*ABHD5/CGI-58 (**Fig. 5A**). Whereas *Mm*ATGL and Bmm/*Dm*ATGL showed basal TG hydrolase activity, lysates from cells expressing *Mm*ABHD5/CGI-58 or Puml did not exceed the lipolytic activities of cells expressing β-galactosidase (negative control). Combinatorial assays (Fig. 5B) confirmed the well-established activation of *Mm*ATGL by *Mm*ABHD5/CGI-58 (12). As negative control, *Mm*ATGL was coincubated with β-galactosidase. In contrast, basal Bmm TG activity was not potentiated by the analogous coincubation with Puml (Fig. 5B). Cross-species combinations of *Mm*ATGL with Puml or Bmm with *Mm*ABHD5/CGI-58 did not indicate any increase in TG lipase activity (Fig. 5B). Collectively, these in vitro data do not support an evolutionarily conserved TG mobilization module consisting of ATGL and ABHD4/5 proteins in flies.

Pummelig is a phospholipase

The Puml protein contains an α/β-hydrolase domain with an active catalytic lipase motif (Fig. 1A, supplemental Fig. S1B) and was previously reported to be a functional esterase in the adult *Drosophila* fat body (47).

To characterize the enzymatic function of Puml, we expressed wild-type Puml and Puml variants with point mutations (Fig. 5C) in the predicted catalytically relevant motifs in High Five™ insect cells, and performed a substrate scan using cell lysates on various ester bond-containing lipids in comparison to control cells expressing β-galactosidase. Pummelig lipase released FAs from phosphatidic acid (PA), *N*-acylphosphatidylethanolamine (NAPE), and phosphatidylglycerol (PG) (Fig. 5D). In contrast, glycerolipids like TGs with various FA side chain lengths as well as diolein and monoolein were not hydrolyzed by Puml (Fig. 5D). Point mutations in any one of the two predicted catalytically relevant motifs (i.e., the catalytic center nucleophile GxSxG and the Hx_4D motif; Fig. 5C) of Puml abrogated the lipolytic activity of Puml on all substrates tested. Collectively, these data identify Pummelig as a phospholipase with a substrate spectrum that overlaps with mammalian ABHD4 (48). Puml exhibited a pH optimum at ~7 (Fig. 5E). Substrate saturation measurements with PA revealed a K_m of ~0.78 mM (V_{max} = 1.49 μmol/h/mg protein) and a drastically lower activity on *sn*-1-oleoyl-lysoPA (Fig. 5F). Further experiments revealed that Puml degrades PA in a dose- and time-dependent manner (Fig. 5G, H).

Pummelig protein localizes to LDs, mitochondria, and peroxisomes

In support of Puml being a bona fide LD-associated protein, the endogenous protein had been found on embryonic LDs (37), and protein correlation profiling in *Drosophila* S2 cell culture identified overexpressed Puml::mCherry as an exclusive LD resident (49). We generated a genomic rescue transgene construct composed of a C-terminally mCherry-tagged Puml under the endogenous promoter control (Fig. 1C) to demonstrate that the fusion protein localizes on the LD surface of adult fat body cells (**Fig. 6A–C**). This finding leaves the possibility that the Puml phospholipase acts directly on the phospholipid monolayer covering the LD surface. Importantly, however, next to LDs, Puml::mCherry localized to additional cellular compartments (Fig. 6C). Overexpression of *puml::GFP* in MTs not only detected the fusion protein in ring-like structures characteristic for LDs (blue arrow in Fig. 6F), but also a substantial fraction of Puml::GFP colocalized with a mitochondrial marker in fly kidney cells (Fig. 6D–F; yellow arrow in Fig. 6F). Importantly, the average size of MT mitochondria in *puml*^{1} flies was significantly increased compared with control flies (Fig. 6G). Notably, mitochondrial anomalies have also been reported in ABHD5/CGI-58 mutant mice (50). Yet, another fraction of Puml::GFP did not exhibit a ring-like pattern and was not colocalized with mitochondria (magenta arrow in Fig. 6F). Collectively, Puml localized to various intracellular organelles, including LDs and mitochondria. This localization is important for their structural integrity and might be of functional relevance for these organelles.

Analysis of transgenic flies coexpressing *puml::mCherry* and an *eYFP* reporter targeted to peroxisomes revealed that a small fraction of Puml::mCherry (Fig. 6K) localized to the majority of peroxisomes detectable in MT cells (Fig. 6L). As mitochondria and peroxisomes are sites of cellular FA β-oxidation, we performed TG FA profiling of MTs on two different lipidomic platforms to address a possible implication of *puml* in this process. Next to the general increase of all TG species in *puml*^{1} flies (Fig. 4G, supplemental Fig. S5), relative TG species abundance analyses indicated a trend to TG species with longer and more unsaturated FA in *puml*^{1} flies (supplemental Figs. S4, S5), which deserves future research attention. Interestingly, these changes in the TG FA profile are reminiscent of peroxisomal biogenesis mutants such as *pex3* (32, 51).

ASBMB JOURNAL OF LIPID RESEARCH

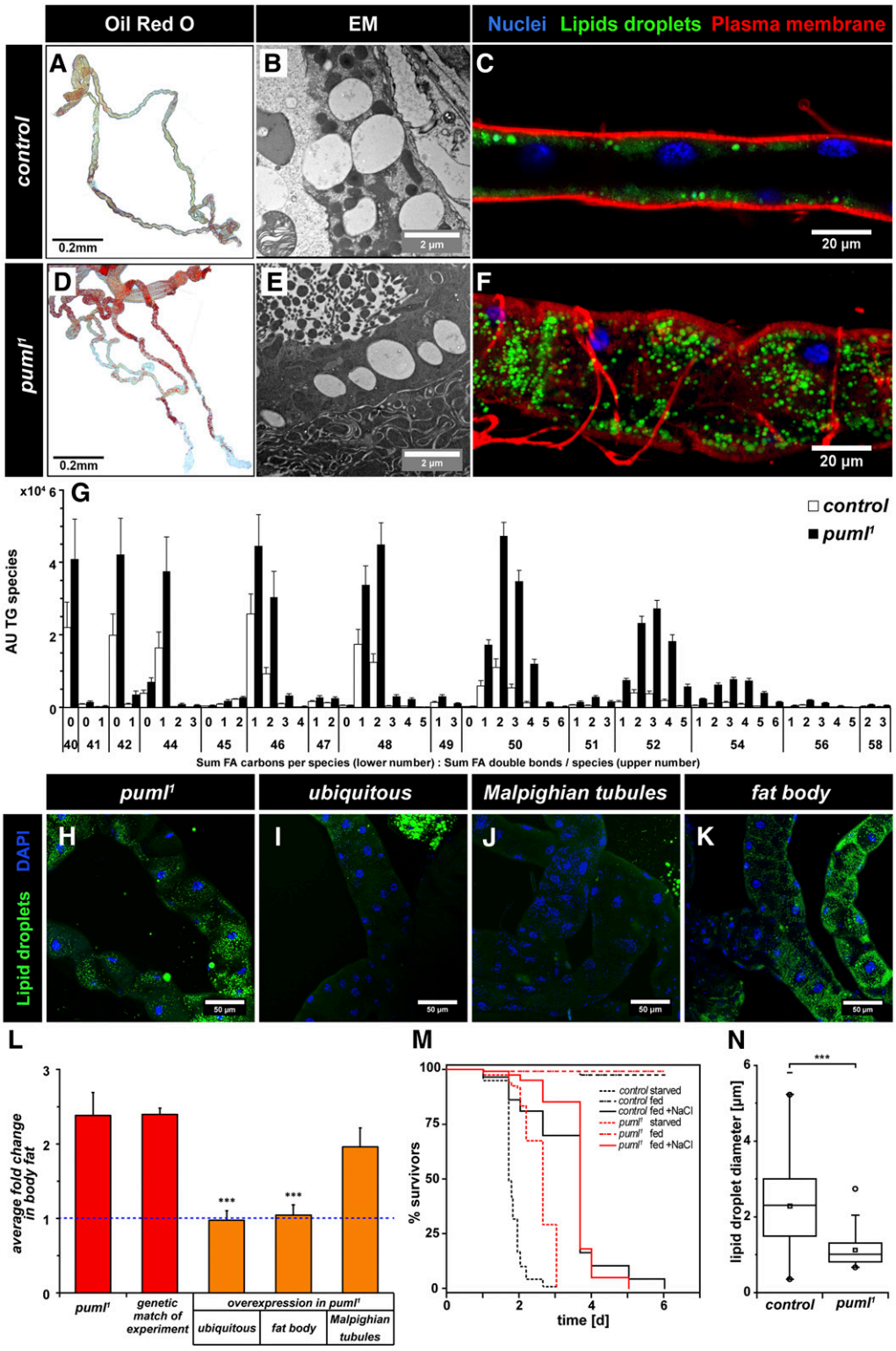

Fig. 4. Ectopic lipid storage and LD structural changes in the MTs of *pummelig* mutant flies. A, D: Ectopic lipid storage in fixed MTs of *puml*^{1} mutant flies compared with controls as detected by Oil Red O staining. B, E: Electron microscopy detects the presence of bona fide LDs as spherical electron-lucent structures in MTs of *puml*^{1} mutant and control flies. C, F: Confirmation of excess LDs in *puml*^{1} mutant MTs compared with control MTs by the lipophilic dye Bodipy493/503 (green). G: General increase of TG species in *puml*^{1} mutants compared with controls detected by TG FA profiling (AU, arbitrary units). Tissue-autonomous function of *puml* for storage lipid control in the MTs. Shown is the reversion of ectopic lipid storage in MTs of *puml*^{1} mutant flies (H) by expressing *puml* ubiquitously (*Act5c>puml*) (I) or specifically in the MTs (*UO>puml*) (J), but not by expression in the fat body (*FB-SNS>puml*) (K). L: Ubiquitous and fat body-targeted expression of *puml* in *puml*^{1} flies restores body fat storage to control levels (blue line). In contrast, the reversion of MT-specific

Taken together, our data suggest that Puml serves a variety of functions in lipid metabolism of flies due to its enzymatic substrate spectrum and due to the association of the protein with various organelles like LDs, mitochondria, and peroxisomes. Collective lack of these functions resulted in an excess of TG storage in the fat body and ectopic lipid storage in MTs. These profound changes in *Drosophila* lipid metabolism correlate with severe physiological phenotypes in *puml*^{1} flies, such as shorter lifespan and reduced physical performance.

DISCUSSION

Our study demonstrates that *pummelig* (*puml*), the single *Drosophila* representative of the *ABHD4/5* lipase gene family, has versatile functions in flies. *puml*^{1} flies are viable but short-lived, exhibit excessive body fat accumulation, and suffer from impaired physical fitness. Despite its structural similarity to mammalian ABHD5/CGI-58, Puml does not stimulate TG lipase activity of Bmm/*Dm*ATGL in vitro. Puml acts as a phospholipase localized on LDs, mitochondria, and peroxisomes. Longevity in flies is a complex trait, and currently it is unknown what causes lifespan reduction in *puml*^{1} flies. One known longevity-promoting factor is spermidine, which extends lifespan in a number of species, including flies, by an autophagy-dependent mechanism (52). Notably, the plant ABHD4/5 family member, *A. thaliana CGI-58*, acts in spermidine biosynthesis (53). Accordingly, an evolutionarily conserved function of *puml* in *Drosophila* polyamine metabolism or a possible involvement in autophagy should be addressed in the future.

The prominent phenotype of *puml*^{1} flies is excessive body fat accumulation. It is likely that increased channeling of ingested sugars toward lipogenesis, at the expense of carbohydrate storage, contributes to this phenotype. However, food intake and energy expenditure are normal in *puml*^{1} flies. This imbalance of energy stores has up- and downsides for the survival of *puml*^{1} flies under environmental challenges, such as starvation or desiccation. Whereas the higher body fat storage warrants extended starvation survival of *puml*^{1} flies, desiccation resistance is reduced. The body water content of *Drosophila* is controlled by the insect renal tissue called MTs (54), which express high levels of *puml* (45, 55). We showed that MTs stored abnormal amounts of neutral lipids in a cell-autonomous manner in flies lacking *puml* function. Accordingly, a potential impairment of the MTs' osmoregulatory function due to the absence of *puml* deserves future research attention, although the salt stress response of *puml*^{1} flies was normal.

Ectopic neutral lipid accumulation in various tissues is the hallmark of mammals missing *ABHD5/CGI-58* gene function (18, 21). The mechanistic basis for this phenotype is the lack of ABHD5/CGI-58 interaction with ATGL (and possibly other lipases), which reduces lipolysis (12). Recently, two conserved amino acids (R299, G328) in the C-terminal region shared by vertebrate ABHD5 homologs, but not by ABHD4 proteins (supplemental Fig. S1B), were shown to be crucial for the functional interaction with ATGL (27). Remarkably, substitution of just these two amino acids is sufficient to capacitate rat ABHD4 as an ATGL activator similar to ABHD5 (27). Although these two amino acids are sequence-conserved in *Drosophila* (supplemental Fig. S1B), Puml did not stimulate ATGL hydrolase activity in vitro, neither of mammalian ATGL nor of the *Dm*ATGL-ortholog Bmm. Conversely, mammalian ABHD5 also failed to stimulate Bmm lipase activity. Collectively, these data suggest that, in contrast to the evolutionary ancient role of ATGL family lipases in storage lipid mobilization, ABHD family proteins are a more recent addition to ATGL regulation. This hypothesis gains further support by the fact that a critical tyrosine residue in the Hx_4D-motif of mammalian ABHD5/CGI-58 is not conserved in Puml (supplemental Fig. S1B). In rat ABHD5/CGI-58, this tyrosine residue (Y330) is essential to bind long-chain acyl-CoAs (56), which in turn promotes the interaction with LD-associated perilipins to negatively regulate lipolysis (16, 57).

While Puml is a LD-associated protein, our data do not support an accessory function of Puml in Bmm-mediated lipolysis on the LD surface comparable to ABHD5/CGI-58 stimulating ATGL. In vivo, a broad range of TG species, including TG 54:3 (largely representing triolein), accumulated in the MTs of *puml*^{1} flies (Fig. 4G). Comparably, the TG composition of *bmm*^{1} flies resembles the changes observed in *puml*^{1} flies (supplemental Fig. S6). This finding equally supports a cooperative interaction of Puml and Bmm in a CGI-58/ATGL-like manner, or a Bmm-independent function of Puml, such as remodeling of the LD phospholipid layer.

A weak lysophosphatic acid acyl transferase (LPAAT) had been reported for murine (58) and plant (59) ABHD5/CGI-58. However, this LPAAT activity, presumably mediated by the Hx_4D-motif, has been dismissed (60, 61). Consistently, unlike mammalian ABHD5/CGI-58, Puml contains a functional catalytic site GxSxG-motif characteristic for active lipases (Fig. 5C, supplemental Fig. S1B). Indeed, our earlier study identified Puml (at that time called CG1882) as a fat body lipase by functional proteomics using an activity-based esterase probe (47).

ectopic lipid storage by MT-targeted *puml* expression in *puml*^{1} flies has only a minor effect on the global body fat storage. Plotted are the means ± SEM of fold change of body fat compared with the genetically matched control for *puml*^{1} flies (Student's *t*-test; $***P < 0.001$, $**P < 0.01$). M: No osmotic stress sensitivity caused by ectopic lipid storage in MTs of *puml*^{1} mutant flies. Shown is survival of *puml*^{1} mutants versus control flies under dietary osmotic challenge (4% NaCl; continuous lines), starvation stress (2% agarose; dashed line), and on regular food (dash-dot lines) [flies per condition and genotype (n = 120); log rank-*P* test; $P < 0.001$ for starved flies]. N: The MT LD population of *puml*^{1} flies is of smaller mean size and of more uniform size distribution compared with the MTs from control flies [Mann-Whitney test; number of LDs analyzed by genotype: $n_{puml(1)}$ = 1,715, $n_{w(1,118)}$ = 306; $***P < 0.001$].

ASBMB JOURNAL OF LIPID RESEARCH

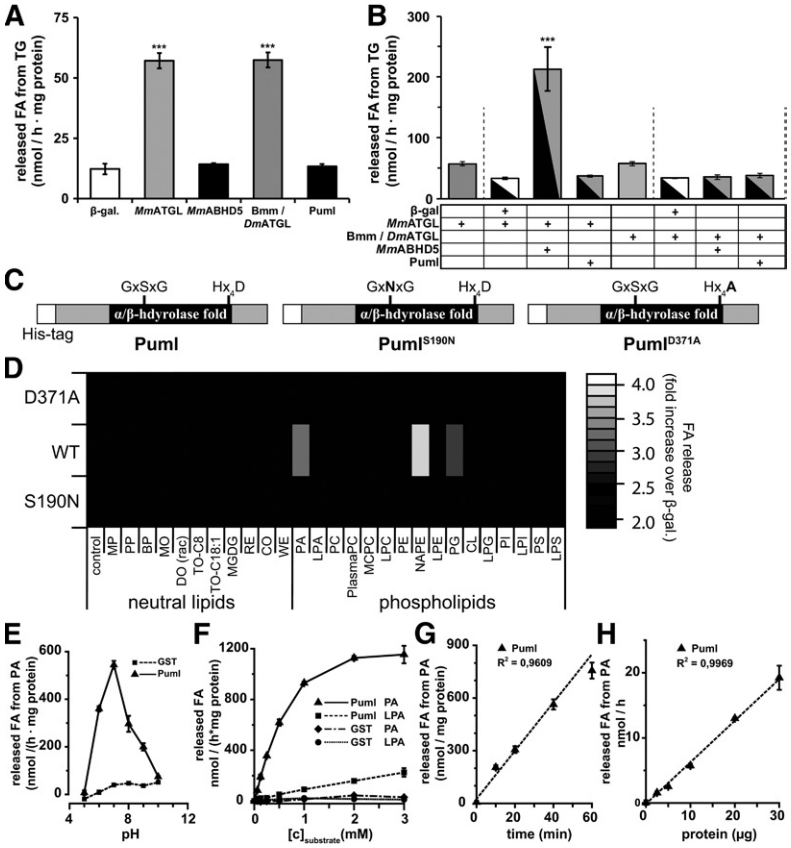

Fig. 5. Structural and enzymatic characterization of Pummelig. A: Basal TG lipase activity of recombinant *Mm*ATGL and Bmm/*Dm*ATGL, but not of *Mm*ABHD5 and Pml, shown by FA release from triolein substrate. Note that β-galactosidase (β-gal.) serves as negative control. B: Stimulated TG lipase activity of *Mm*ATGL by *Mm*ABHD5, but not of Bmm/*Dm*ATGL by Pml. No cross-species stimulation of TG lipase activity upon combining *Mm*ATGL plus Pml or Bmm/*Dm*ATGL plus *Mm*ABHD5. Note that two-component mixtures contain only half of the amount of *Mm*ATGL and Bmm/*Dm*ATGL compared with the activity measurements of *Mm*ATGL and Bmm/*Dm*ATGL alone. C: Schematic of the recombinant protein Pml, the predicted catalytic nucleophile motif mutant Pml^{S190N}, and the predicted acyltransferase motif mutant Pml^{D371A}. Black boxes represent the α/β-hydrolase fold domain, gray boxes the N- and C-terminal regions of Pml, and white boxes the N-terminal His-tag of the fusion proteins. D: Pml is a phospholipase with no activity on neutral lipids. Substrate screening with WT Pml and Pml catalytic motif mutants (D371A and S190N) expressed in insect cells. Data show mean fold increase of FA release from diverse lipid substrates in comparison to cells expressing β-galactosidase (lower cut-off = 2). Pml hydrolyzes PA, NAPE, and PG (for description of all substrates tested; see the supplemental data). Note the lack of hydrolase activity for both of the catalytic motif mutants on any of the tested substrates. E: pH dependence of Pml tested with PA reveals an optimum at neutral to slightly acid pH. F: Substrate saturation assay of Pml using PA and lyso-PA shows a clear preference toward DG-lipid PA. Saturation of Pml with PA was achieved at ~2 mM (K_m = 0.71 mM, V_{max} = 1.49 μmol/h/mg protein). Time-dependent (G) and dose-dependent (H) hydrolysis of PA by cell lysates overexpressing Pml. Note that values were normalized to lysates with overexpressed glutathione *S*-transferase (GST). A, B, E–H: Plotted are the means ± SEM; Mann-Whitney test; ***$P < 0.001$. Statistical tests were performed using following controls: β-gal in D; *Mm*ATGL or Bmm/*Dm*ATGL + β-gal in A and B.

The substrate profiling presented here identifies Pml as a phospholipase without significant hydrolase activity on neutral lipids. Therefore, the excessive storage lipid accumulation in *pml*[1] flies is unlikely caused by an autonomous TG hydrolysis defect, but is rather an indirect consequence of lipid metabolism imbalance in flies lacking Pml function.

Our current understanding on how the absence of Pml causes neutral lipid accumulation is limited by two factors: on the one hand by the unknown or pleiotrophic effects in vivo of the lipids, which are substrates for Pml in vitro, and on the other hand by the multifaceted intracellular localization of the Pml protein.

Interestingly, similar to mammalian ABHD4 (26, 48), Pml hydrolyzes the endocannabinoid precursor NAPE at neutral to slightly acid pH (supplemental Fig. S7). However, its converted form *N*-acylethanolamine (NAE) 20:4 is not endogenously present in *Drosophila*. As the endocannabinoid receptor CB1 is not present in *Drosophila* either, it is surprising that endocannabinoids like NAE 16:0, 18:0, and 18:1 can be found in flies (62). Additionally, these endocannabinoids in *Drosophila* act as hedgehog ligands and directly interact with Smoothened (Smo) at physiological concentrations (62, 63). As hedgehog signaling modulates energy metabolism in flies (64), endocannabinoid

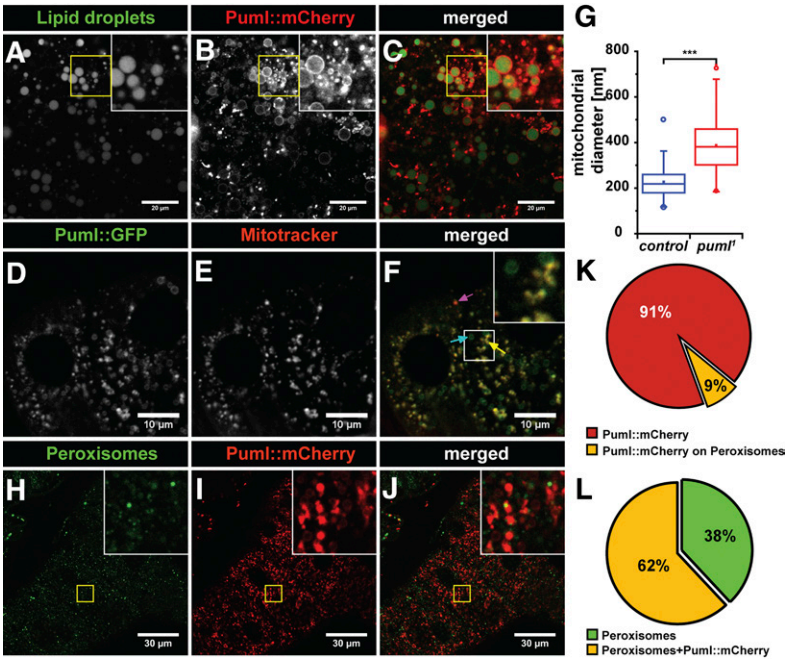

Fig. 6. In vivo localization of Puml fusion proteins on LDs, mitochondria, and peroxisomes. A–C: LD association of Puml::mCherry fusion protein (expressed from the genomic rescue construct; see Fig. 1C) in adult fat body cells. Fluorescence optical sections detect the fusion protein (B) in ring-like structures surrounding LDs (A). Note that a substantial fraction of Puml::mCherry is not associated with LDs. D–F: Mitochondrial localization of a fraction of Puml::eGFP (expressed under endogenous promotor control) in MTs. Fluorescence optical sections detect colocalization (F) of the fusion protein (D) with mitochondria labeled with MitoTracker (E). Note that next to mitochondria (yellow arrow in F), the fusion protein also localizes to MT LDs (blue arrow in F) and to other compartments (magenta arrow in F). G: Enlarged mitochondria in MTs of *puml*^{1} flies compared with controls. H–J: Peroxisomal localization of a minor fraction (K) of Puml::mCherry in MTs. Fluorescence optical sections detect colocalization of the Puml::mCherry fusion protein (I) with the peroxisomal marker protein eYFP::Pts1 (H, L).

metabolism in *puml*^{1} flies might be disturbed. Although, in mice, NAPE-PLD provides an alternative pathway to generate and compensate for NAE and anandamide synthesis in ABHD4 knockout mice (48), it is currently not known whether this pathway is evolutionarily conserved in flies. In mice, NAPE 16:0 is produced and secreted from the gut, especially after high-fat meals, lowering locomotor activity and food intake (65). Presuming an evolutionarily conserved endocannabinoid-based mechanism for sensing the nutritional value and composition of food, one would expect alterations in the behavior of *puml*^{1} flies. However, *puml*^{1} flies are normophagic and display no obvious locomotion phenotype. Additionally, overall hedgehog signaling (62, 63, 66) appears not to be impaired in *puml*^{1} flies, as no obvious developmental defects can be observed, and *puml*^{1} flies are fertile. The question of whether Puml affects NAPE and consecutively NAE metabolism in flies should be addressed in further studies.

The lipid mediator PA is a possible link between the *puml*^{1} phenotype and the enzymatic activity of the protein, as Puml hydrolyzes PA in vitro. High levels of PA cause increased generation of TGs in mammals (28, 67). Additionally, PA negatively regulates the cellular energy sensor, AMPK, which subsequently causes reduced FA import into mitochondria and decreased mitochondrial biogenesis (68, 69). At the same time, PA stabilizes the TORC1-complex (67). The possible AMPK and TORC1 modulation mediated by changes in PA levels in *puml*^{1} flies could explain the observed higher lipogenesis and lower carbohydrate storage. Notably, ABHD5/CGI-58 knockdown mice suffering from hepatic steatosis have increased levels of some PA species and accumulate (~10-fold) PG (28), another in vitro substrate of Puml.

An intrinsic lysophosphatidylglycerol acyltransferase (LPGAT) activity had been reported for murine ABHD5/CGI-58 (70). However, this is currently under debate, as PGs are actually increased in hepatocytes of ABHD5 knockdown mice (28), and a more recent publication could not confirm this activity for mouse and plant ABHD5 (61).

PA and PG are precursors for cardiolipin (CL), a highly important lipid nearly exclusively found on mitochondria. CL has multiple roles on these organelles, as it stabilizes proteins needed for oxidative phosphorylation, is a proton trap within mitochondrial membranes, is involved in mitochondria-induced apoptosis, and shapes mitochondrial membrane dynamics [for review see (71)]. As Puml localizes on mitochondria as well, it might be involved in modulating the generation of CL by limiting the locally available PA and PG pool for mitochondria, changing their properties. This also might provide a link for the observation that a knockdown of ABHD5/CGI-58 in SW620 and HCT116 cells suppresses the AMPKα-p53 pathway and leads to a metabolic shift toward aerobic glycolysis (Warburg effect) and to lipid accumulation (72). Additionally, CL serves as a substrate for Mito-PLD locally generating PA, critical for mitochondrial fusion. As Puml hydrolyzes PA, LPA, and PG, and is localized on mitochondria, this might provide an explanation for the overall enlarged mitochondria found in *puml*^{1} flies. Missing *puml* gene function may alter local PA and PG on mitochondria, subsequently leading to changed CL levels, and missing PA hydrolysis activity of Puml may cause increased PA levels in mitochondrial membranes leading to increased fusion.

Furthermore, future attention should focus on a possible interaction of Puml with lipin and AGPAT3. All three enzymes are LD residents (73), with the latter two directly involved in the lipogenesis pathway. While AGPAT3 is required for PA production from LPA, lipin is consecutively needed for DG synthesis from PA (PA-phosphatase; PAP activity). Lipin is of especially high interest here, as it regulates lipid metabolism directly by generating DG via its PAP activity and also by acting as a transcription factor in the

ASBMB JOURNAL OF LIPID RESEARCH

nucleus (74). Interestingly, downstream targets of lipin (as a transcription factor) are lipolytic (like PPARα) and oxidative phosphorylation genes, whereas lipogenic genes (like FASN) are suppressed (75). Additionally, lipin interacts and is activated by TORC1, preventing it from translocation into the nucleus (74). As the TORC1 complex is stabilized by PA (76), this might provide a positive feedback loop under nutrition, stimulating lipogenesis. Therefore, Puml might limit the locally available amount of PA for lipin and thereby indirectly modulate the activity of lipin. Hence, absence of *puml* would enhance the lipogenic feedback loop leading to increased amounts of TGs, an effect observed in *puml*^{1} flies. This would also explain why lipolysis is not affected in *puml*^{1} flies; as without PA, lipin would be able enhance lipolysis as a transcriptional cofactor. Therefore, a possible interaction of Puml with lipin should be addressed in future studies.

Besides possible negative effects on mitochondrial function, the peroxisomal localization of Puml::mCherry, a feature shared with the ABHD4/5 homolog from *A. thaliana* (77), might be of functional relevance for TG turnover. In support of this, the TG FA composition of *puml*^{1} flies is shifted toward longer and more unsaturated FAs, reminiscent of flies defective in peroxisomal biogenesis (32, 78). Also, both *puml* and peroxisomal mutant flies share decreased lifespan and impaired startle-induced climbing activity (32, 78). Finally, flies mutant for the core peroxisomal genes, *pex2* and *pex16*, store less glycogen (51), one additional phenotype shared by *puml*^{1} flies. Collectively, these data support a peroxisomal function of Puml, regardless of the protein having no prototypic peroxisomal targeting signal (79), which predicts the localization of Puml to these organelles to be mediated by a currently unknown binding partner.

Key to the understanding of the Puml intracellular localization complexity might be the fact that *puml* encodes different predicted protein isoforms, which differ in their N termini (80). For example, the longest Puml isoform (Puml-PA) has an extended N terminus that contains multiple phenylalanine ($F^{52,53}$) and tryptophan ($W^{55,57,61}$) residues. This is reminiscent of the tryptophan-rich N-terminal peptide of ABHD5/CGI-58, which is essential for the LD anchoring of the protein (81, 82).

Taken together, our data suggest that Puml serves a variety of functions in lipid metabolism of flies due to its enzymatic substrate spectrum and due to the association of the protein with various organelles like LDs, mitochondria, and peroxisomes. Collective lack of these functions results in an excess of TG storage in the fat body and ectopic lipid storage in the MTs. These profound changes in *Drosophila* lipid metabolism correlate with severe physiological phenotypes in *puml*^{1} flies, such as shorter lifespan and reduced physical performance. Future research efforts addressing the underlying molecular and physiological mechanisms are necessary. TG storage in the insect kidney indicates ancestral metabolic functions of this gene family with relevance for a more comprehensive understanding of mammalian ABHD4 and ABHD5/CGI-58 proteins.

The authors thank Drs. J. E. Faust, J. Dow, and J. A. McNew for providing fly stocks; Drs. A. Lass, A. Hildebrandt, and I. Berger for providing plasmids; and R. Schuh for support during the writing phase of the manuscript.

REFERENCES

1. Bailey, A. P., G. Koster, C. Guillermier, E. M. Hirst, J. I. MacRae, C. P. Lechene, A. D. Postle, and A. P. Gould. 2015. Antioxidant role for lipid droplets in a stem cell niche of Drosophila. *Cell.* **163:** 340–353.
2. Ghosh, A. K., N. Chauhan, S. Rajakumari, G. Daum, and R. Rajasekharan. 2009. At4g24160, a soluble acyl-coenzyme A-dependent lysophosphatidic acid acyltransferase. *Plant Physiol.* **151:** 869–881.
3. Grönke, S., M. Beller, S. Fellert, H. Ramakrishnan, H. Jäckle, and R. P. Kühnlein. 2003. Control of fat storage by a Drosophila PAT domain protein. *Curr. Biol.* **13:** 603–606.
4. Beller, M., A. V. Bulankina, H. H. Hsiao, H. Urlaub, H. Jackle, and R. P. Kuhnlein. 2010. Perilipin-dependent control of lipid droplet structure and fat storage in Drosophila. *Cell Metab.* **12:** 521–532.
5. Teixeira, L. s., C. Rabouille, P. Rørth, A. Ephrussi, and N. F. Vanzo. 2003. Drosophila perilipin/ADRP homologue Lsd2 regulates lipid metabolism. *Mech. Dev.* **120:** 1071–1081.
6. Bi, J., Y. Xiang, H. Chen, Z. Liu, S. Grönke, R. P. Kühnlein, and X. Huang. 2012. Opposite and redundant roles of the two Drosophila perilipins in lipid mobilization. *J. Cell Sci.* **125:** 3568–3577.
7. Buszczak, M., X. Lu, W. A. Segraves, T. Y. Chang, and L. Cooley. 2002. Mutations in the midway gene disrupt a Drosophila acyl coenzyme A:diacylglycerol acyltransferase. *Genetics.* **160:** 1511–1518.
8. Grönke, S., G. Müller, J. Hirsch, S. Fellert, A. Andreou, T. Haase, H. Jäckle, and R. P. Kühnlein. 2007. Dual lipolytic control of body fat storage and mobilization in Drosophila. *PLoS Biol.* **5:** e137.
9. Grönke, S., A. Mildner, S. Fellert, N. Tennagels, S. Petry, G. Müller, H. Jäckle, and R. P. Kühnlein. 2005. Brummer lipase is an evolutionary conserved fat storage regulator in Drosophila. *Cell Metab.* **1:** 323–330.
10. Zimmermann, R., J. G. Strauss, G. Haemmerle, G. Schoiswohl, R. Birner-Gruenberger, M. Riederer, A. Lass, G. Neuberger, F. Eisenhaber, A. Hermetter, et al. 2004. Fat mobilization in adipose tissue is promoted by adipose triglyceride lipase. *Science.* **306:** 1383–1386.
11. Haemmerle, G., A. Lass, R. Zimmermann, G. Gorkiewicz, C. Meyer, J. Rozman, G. Heldmaier, R. Maier, C. Theussl, S. Eder, et al. 2006. Defective lipolysis and altered energy metabolism in mice lacking adipose triglyceride lipase. *Science.* **312:** 734–737.
12. Lass, A., R. Zimmermann, G. Haemmerle, M. Riederer, G. Schoiswohl, M. Schweiger, P. Kienesberger, J. G. Strauss, G. Gorkiewicz, and R. Zechner. 2006. Adipose triglyceride lipase-mediated lipolysis of cellular fat stores is activated by CGI-58 and defective in Chanarin-Dorfman syndrome. *Cell Metab.* **3:** 309–319.
13. Subramanian, V., A. Rothenberg, C. Gomez, A. W. Cohen, A. Garcia, S. Bhattacharyya, L. Shapiro, G. Dolios, R. Wang, M. P. Lisanti, et al. 2004. Perilipin A mediates the reversible binding of CGI-58 to lipid droplets in 3T3-L1 adipocytes. *J. Biol. Chem.* **279:** 42062–42071.
14. Yamaguchi, T., N. Omatsu, S. Matsushita, and T. Osumi. 2004. CGI-58 interacts with perilipin and is localized to lipid droplets. Possible involvement of CGI-58 mislocalization in Chanarin-Dorfman syndrome. *J. Biol. Chem.* **279:** 30490–30497.
15. Granneman, J. G., H. P. Moore, R. L. Granneman, A. S. Greenberg, M. S. Obin, and Z. Zhu. 2007. Analysis of lipolytic protein trafficking and interactions in adipocytes. *J. Biol. Chem.* **282:** 5726–5735.
16. Granneman, J. G., H. P. Moore, R. Krishnamoorthy, and M. Rathod. 2009. Perilipin controls lipolysis by regulating the interactions of AB-hydrolase containing 5 (Abhd5) and adipose triglyceride lipase (Atgl). *J. Biol. Chem.* **284:** 34538–34544.
17. Fischer, J., C. Lefevre, E. Morava, J. M. Mussini, P. Laforet, A. Negre-Salvayre, M. Lathrop, and R. Salvayre. 2007. The gene encoding adipose triglyceride lipase (PNPLA2) is mutated in neutral lipid storage disease with myopathy. *Nat. Genet.* **39:** 28–30.
18. Lefèvre, C., F. Jobard, F. Caux, B. Bouadjar, A. Karaduman, R. Heilig, H. Lakhdar, A. Wollenberg, J. L. Verret, J. Weissenbach, et al. 2001. Mutations in CGI-58, the gene encoding a new protein of the esterase/lipase/thioesterase subfamily, in Chanarin-Dorfman syndrome. *Am. J. Hum. Genet.* **69:** 1002–1012.
19. Brown, A. L., and J. Mark Brown. 2017. Critical roles for alpha/beta hydrolase domain 5 (ABHD5)/comparative gene identification-58

(CGI-58) at the lipid droplet interface and beyond. *Biochim. Biophys. Acta Mol. Cell Biol. Lipids.* **1862 (10 Pt B):** 1233–1241.
20. Cerk, I. K., L. Wechselberger, and M. Oberer. 2018. Adipose triglyceride lipase regulation: an overview. *Curr. Protein Pept. Sci.* **19:** 221–233.
21. Radner, F. P., I. E. Streith, G. Schoiswohl, M. Schweiger, M. Kumari, T. O. Eichmann, G. Rechberger, H. C. Koefeler, S. Eder, S. Schauer, et al. 2010. Growth retardation, impaired triacylglycerol catabolism, hepatic steatosis, and lethal skin barrier defect in mice lacking comparative gene identification-58 (CGI-58). *J. Biol. Chem.* **285:** 7300–7311.
22. Hofer, P., A. Boeszoermenyi, D. Jaeger, U. Feiler, H. Arthanari, N. Mayer, F. Zehender, G. Rechberger, M. Oberer, R. Zimmermann, et al. 2015. Fatty acid-binding proteins interact with comparative gene identification-58 linking lipolysis with lipid ligand shuttling. *J. Biol. Chem.* **290:** 18438–18453.
23. Yamaguchi, T., N. Omatsu, E. Morimoto, H. Nakashima, K. Ueno, T. Tanaka, K. Satouchi, F. Hirose, and T. Osumi. 2007. CGI-58 facilitates lipolysis on lipid droplets but is not involved in the vesiculation of lipid droplets caused by hormonal stimulation. *J. Lipid Res.* **48:** 1078–1089.
24. Kien, B., S. Grond, G. Haemmerle, A. Lass, T. O. Eichmann, and F. P. W. Radner. 2018. ABHD5 stimulates PNPLA1-mediated omega-*O*-acylceramide biosynthesis essential for a functional skin permeability barrier. *J. Lipid Res.* **59:** 2360–2367.
25. Simpson, C. D., R. Hurren, D. Kasimer, N. MacLean, Y. Eberhard, T. Ketela, J. Moffat, and A. D. Schimmer. 2012. A genome wide shRNA screen identifies alpha/beta hydrolase domain containing 4 (ABHD4) as a novel regulator of anoikis resistance. *Apoptosis.* **17:** 666–678.
26. Simon, G. M., and B. F. Cravatt. 2006. Endocannabinoid biosynthesis proceeding through glycerophospho-N-acyl ethanolamine and a role for alpha/beta-hydrolase 4 in this pathway. *J. Biol. Chem.* **281:** 26465–26472.
27. Sanders, M. A., H. Zhang, L. Mladenovic, Y. Y. Tseng, and J. G. Granneman. 2017. Molecular Basis of ABHD5 Lipolysis Activation. *Sci. Rep.* **7:** 42589.
28. Brown, J. M., J. L. Betters, C. Lord, Y. Ma, X. Han, K. Yang, H. M. Alger, J. Melchior, J. Sawyer, R. Shah, et al. 2010. CGI-58 knockdown in mice causes hepatic steatosis but prevents diet-induced obesity and glucose intolerance. *J. Lipid Res.* **51:** 3306–3315.
29. Goeritzer, M., S. Schlager, B. Radovic, C. T. Madreiter, S. Rainer, G. Thomas, C. C. Lord, J. Sacks, A. L. Brown, N. Vujic, et al. 2014. Deletion of CGI-58 or adipose triglyceride lipase differently affects macrophage function and atherosclerosis. *J. Lipid Res.* **55:** 2562–2575.
30. Lord, C. C., J. L. Betters, P. T. Ivanova, S. B. Milne, D. S. Myers, J. Madenspacher, G. Thomas, S. Chung, M. Liu, M. A. Davis, et al. 2012. CGI-58/ABHD5-derived signaling lipids regulate systemic inflammation and insulin action. *Diabetes.* **61:** 355–363.
31. Lord, C. C., and J. M. Brown. 2012. Distinct roles for alpha-beta hydrolase domain 5 (ABHD5/CGI-58) and adipose triglyceride lipase (ATGL/PNPLA2) in lipid metabolism and signaling. *Adipocyte.* **1:** 123–131.
32. Faust, J. E., A. Manisundaram, P. T. Ivanova, S. B. Milne, J. B. Summerville, H. A. Brown, M. Wangler, M. Stern, and J. A. McNew. 2014. Peroxisomes are required for lipid metabolism and muscle function in Drosophila melanogaster. *PLoS One.* **9:** e100213.
33. Lee, J. H., J. Kong, J. Y. Jang, J. S. Han, Y. Ji, J. Lee, and J. B. Kim. 2014. Lipid droplet protein LID-1 mediates ATGL-1-dependent lipolysis during fasting in Caenorhabditis elegans. *Mol. Cell. Biol.* **34:** 4165–4176.
34. Xie, M., and R. Roy. 2015. The causative gene in Chanarian Dorfman syndrome regulates lipid droplet homeostasis in C. elegans. *PLoS Genet.* **11:** e1005284.
35. Gáliková, M., M. Diesner, P. Klepsatel, P. Hehlert, Y. Xu, I. Bickmeyer, R. Predel, and R. P. Kühnlein. 2015. Energy homeostasis control in Drosophila adipokinetic hormone mutants. *Genetics.* **201:** 665–683.
36. Bellen, H. J., R. W. Levis, G. Liao, Y. He, J. W. Carlson, G. Tsang, M. Evans-Holm, P. R. Hiesinger, K. L. Schulze, G. M. Rubin, et al. 2004. The BDGP gene disruption project: single transposon insertions associated with 40% of Drosophila genes. *Genetics.* **167:** 761–781.
37. Hildebrandt, A., I. Bickmeyer, and R. P. Kühnlein. 2011. Reliable Drosophila body fat quantification by a coupled colorimetric assay. *PLoS One.* **6:** e23796.
38. Baumbach, J., P. Hummel, I. Bickmeyer, K. M. Kowalczyk, M. Frank, K. Knorr, A. Hildebrandt, D. Riedel, H. Jäckle, and R. P. Kühnlein. 2014. A Drosophila in vivo screen identifies store-operated calcium entry as a key regulator of adiposity. *Cell Metab.* **19:** 331–343.
39. Yatsenko, A. S., A. K. Marrone, M. M. Kucherenko, and H. R. Shcherbata. 2014. Measurement of metabolic rate in Drosophila using respirometry. *J. Vis. Exp.* (88): e51681.
40. Katewa, S. D., F. Demontis, M. Kolipinski, A. Hubbard, M. S. Gill, N. Perrimon, S. Melov, and P. Kapahi. 2012. Intramyocellular fatty-acid metabolism plays a critical role in mediating responses to dietary restriction in Drosophila melanogaster. *Cell Metab.* **16:** 97–103.
41. Schweiger, M., T. O. Eichmann, U. Taschler, R. Zimmermann, R. Zechner, and A. Lass. 2014. Measurement of lipolysis. *Methods Enzymol.* **538:** 171–193.
42. Pribasnig, M. A., I. Mrak, G. F. Grabner, U. Taschler, O. Knittelfelder, B. Scherz, T. O. Eichmann, C. Heier, L. Grumet, J. Kowaliuk, et al. 2015. α/β Hydrolase domain-containing 6 (ABHD6) degrades the late endosomal/lysosomal lipid bis(monoacylglycero)phosphate. *J. Biol. Chem.* **290:** 29869–29881.
43. Heier, C., U. Taschler, M. Radulovic, P. Aschauer, T. O. Eichmann, S. Grond, H. Wolinski, M. Oberer, R. Zechner, S. D. Kohlwein, et al. 2016. Monoacylglycerol lipases act as evolutionarily conserved regulators of non-oxidative ethanol metabolism. *J. Biol. Chem.* **291:** 11865–11875.
44. Hummel, J., S. Segu, Y. Li, S. Irgang, J. Jueppner, and P. Giavalisco. 2011. Ultra performance liquid chromatography and high resolution mass spectrometry for the analysis of plant lipids. *Front. Plant Sci.* **2:** 54.
45. Robinson, S. W., P. Herzyk, J. A. Dow, and D. P. Leader. 2013. FlyAtlas: database of gene expression in the tissues of Drosophila melanogaster. *Nucleic Acids Res.* **41:** D744–D750.
46. Huylmans, A. K., and J. Parsch. 2014. Population- and sex-biased gene expression in the excretion organs of Drosophila melanogaster. *G3 (Bethesda).* **4:** 2307–2315.
47. Birner-Gruenberger, R., I. Bickmeyer, J. Lange, P. Hehlert, A. Hermetter, M. Kollroser, G. N. Rechberger, and R. P. Kühnlein. 2012. Functional fat body proteomics and gene targeting reveal in vivo functions of Drosophila melanogaster α-esterase-7. *Insect Biochem. Mol. Biol.* **42:** 220–229.
48. Lee, H. C., G. M. Simon, and B. F. Cravatt. 2015. ABHD4 regulates multiple classes of N-acyl phospholipids in the mammalian central nervous system. *Biochemistry.* **54:** 2539–2549.
49. Krahmer, N., M. Hilger, N. Kory, F. Wilfling, G. Stoehr, M. Mann, R. V. Farese, Jr., and T. C. Walther. 2013. Protein correlation profiles identify lipid droplet proteins with high confidence. *Mol. Cell. Proteomics.* **12:** 1115–1126.
50. Zierler, K. A., D. Jaeger, N. M. Pollak, S. Eder, G. N. Rechberger, F. P. Radner, G. Woelkart, D. Kolb, A. Schmidt, M. Kumari, et al. 2013. Functional cardiac lipolysis in mice critically depends on comparative gene identification-58. *J. Biol. Chem.* **288:** 9892–9904.
51. Wangler, M. F., Y. H. Chao, V. Bayat, N. Giagtzoglou, A. B. Shinde, N. Putluri, C. Coarfa, T. Donti, B. H. Graham, J. E. Faust, et al. 2017. Peroxisomal biogenesis is genetically and biochemically linked to carbohydrate metabolism in Drosophila and mouse. *PLoS Genet.* **13:** e1006825.
52. Eisenberg, T., H. Knauer, A. Schauer, S. Buttner, C. Ruckenstuhl, D. Carmona-Gutierrez, J. Ring, S. Schroeder, C. Magnes, L. Antonacci, et al. 2009. Induction of autophagy by spermidine promotes longevity. *Nat. Cell Biol.* **11:** 1305–1314.
53. Park, S., J. Keereetaweep, C. N. James, S. K. Gidda, K. D. Chapman, R. T. Mullen, and J. M. Dyer. 2014. CGI-58, a key regulator of lipid homeostasis and signaling in plants, also regulates polyamine metabolism. *Plant Signal. Behav.* **9:** e27723.
54. Beyenbach, K. W., H. Skaer, and J. A. Dow. 2010. The developmental, molecular, and transport biology of Malpighian tubules. *Annu. Rev. Entomol.* **55:** 351–374.
55. Wang, J., L. Kean, J. Yang, A. K. Allan, S. A. Davies, P. Herzyk, and J. A. Dow. 2004. Function-informed transcriptome analysis of Drosophila renal tubule. *Genome Biol.* **5:** R69.
56. Sanders, M. A., F. Madoux, L. Mladenovic, H. Zhang, X. Ye, M. Angrish, E. P. Mottillo, J. A. Caruso, G. Halvorsen, W. R. Roush, et al. 2015. Endogenous and synthetic ABHD5 ligands regulate ABHD5-perilipin interactions and lipolysis in fat and muscle. *Cell Metab.* **22:** 851–860.
57. Granneman, J. G., H. P. Moore, E. P. Mottillo, and Z. Zhu. 2009. Functional interactions between Mldp (LSDP5) and Abhd5 in the control of intracellular lipid accumulation. *J. Biol. Chem.* **284:** 3049–3057.
58. Montero-Moran, G., J. M. Caviglia, D. McMahon, A. Rothenberg, V. Subramanian, Z. Xu, S. Lara-Gonzalez, J. Storch, G. M. Carman, and

D. L. Brasaemle. 2010. CGI-58/ABHD5 is a coenzyme A-dependent lysophosphatidic acid acyltransferase. *J. Lipid Res.* **51:** 709–719.
59. Ghosh, A. K., G. Ramakrishnan, C. Chandramohan, and R. Rajasekharan. 2008. CGI-58, the causative gene for Chanarin-Dorfman syndrome, mediates acylation of lysophosphatidic acid. *J. Biol. Chem.* **283:** 24525–24533.
60. McMahon, D., A. Dinh, D. Kurz, D. Shah, G. S. Han, G. M. Carman, and D. Brasaemle. 2014. Comparative gene identification 58 (CGI-58)/α/β hydrolase domain 5 (ABHD5) lacks lysophosphatidic acid acyltransferase activity. *J. Lipid Res.* **55:** 1750–1761.
61. Khatib, A., Y. Arhab, A. Bentebibel, A. Abousalham, and A. Noiriel. 2016. Reassessing the potential activities of plant CGI-58 protein. *PLoS One.* **11:** e0145806.
62. Khaliullina, H., M. Bilgin, J. L. Sampaio, A. Shevchenko, and S. Eaton. 2015. Endocannabinoids are conserved inhibitors of the Hedgehog pathway. *Proc. Natl. Acad. Sci. USA.* **112:** 3415–3420.
63. Khaliullina, H., D. Panakova, C. Eugster, F. Riedel, M. Carvalho, and S. Eaton. 2009. Patched regulates Smoothened trafficking using lipoprotein-derived lipids. *Development.* **136:** 4111–4121.
64. Pospisilik, J. A., D. Schramek, H. Schnidar, S. J. Cronin, N. T. Nehme, X. Zhang, C. Knauf, P. D. Cani, K. Aumayr, J. Todoric, et al. 2010. Drosophila genome-wide obesity screen reveals hedgehog as a determinant of brown versus white adipose cell fate. *Cell.* **140:** 148–160.
65. Gillum, M. P., D. Zhang, X. M. Zhang, D. M. Erion, R. A. Jamison, C. Choi, J. Dong, M. Shanabrough, H. R. Duenas, D. W. Frederick, et al. 2008. N-acylphosphatidylethanolamine, a gut-derived circulating factor induced by fat ingestion, inhibits food intake. *Cell.* **135:** 813–824.
66. Çiçek, I. Ö., S. Karaca, M. Brankatschk, S. Eaton, H. Urlaub, and H. R. Shcherbata. 2016. Hedgehog signaling strength is orchestrated by the mir-310 cluster of microRNAs in response to diet. *Genetics.* **202:** 1167–1183.
67. Foster, D. A., and A. Toschi. 2009. Targeting mTOR with rapamycin: one dose does not fit all. *Cell Cycle.* **8:** 1026–1029.
68. Hardie, D. G. 2011. AMP-activated protein kinase: an energy sensor that regulates all aspects of cell function. *Genes Dev.* **25:** 1895–1908.
69. Mukhopadhyay, S., M. Saqcena, A. Chatterjee, A. Garcia, M. A. Frias, and D. A. Foster. 2015. Reciprocal regulation of AMP-activated protein kinase and phospholipase D. *J. Biol. Chem.* **290:** 6986–6993.
70. Zhang, J., D. Xu, J. Nie, R. Han, Y. Zhai, and Y. Shi. 2014. Comparative gene identification-58 (CGI-58) promotes autophagy as a putative lysophosphatidylglycerol acyltransferase. *J. Biol. Chem.* **289:** 33044–33053.
71. Houtkooper, R. H., and F. M. Vaz. 2008. Cardiolipin, the heart of mitochondrial metabolism. *Cell. Mol. Life Sci.* **65:** 2493–2506.
72. Ou, J., H. Miao, Y. Ma, F. Guo, J. Deng, X. Wei, J. Zhou, G. Xie, H. Shi, B. Xue, et al. 2014. Loss of abhd5 promotes colorectal tumor development and progression by inducing aerobic glycolysis and epithelial-mesenchymal transition. *Cell Reports.* **9:** 1798–1811.
73. Wilfling, F., H. Wang, J. T. Haas, N. Krahmer, T. J. Gould, A. Uchida, J. X. Cheng, M. Graham, R. Christiano, F. Frohlich, et al. 2013. Triacylglycerol synthesis enzymes mediate lipid droplet growth by relocalizing from the ER to lipid droplets. *Dev. Cell.* **24:** 384–399.
74. Schmitt, S., R. Ugrankar, S. E. Greene, M. Prajapati, and M. Lehmann. 2015. Drosophila lipin interacts with insulin and TOR signaling pathways in the control of growth and lipid metabolism. *J. Cell Sci.* **128:** 4395–4406.
75. Finck, B. N., M. C. Gropler, Z. Chen, T. C. Leone, M. A. Croce, T. E. Harris, J. C. Lawrence, Jr., and D. P. Kelly. 2006. Lipin 1 is an inducible amplifier of the hepatic PGC-1alpha/PPARalpha regulatory pathway. *Cell Metab.* **4:** 199–210.
76. Toschi, A., E. Lee, L. Xu, A. Garcia, N. Gadir, and D. A. Foster. 2009. Regulation of mTORC1 and mTORC2 complex assembly by phosphatidic acid: competition with rapamycin. *Mol. Cell. Biol.* **29:** 1411–1420.
77. James, C. N., P. J. Horn, C. R. Case, S. K. Gidda, D. Zhang, R. T. Mullen, J. M. Dyer, R. G. Anderson, and K. D. Chapman. 2010. Disruption of the Arabidopsis CGI-58 homologue produces Chanarin-Dorfman-like lipid droplet accumulation in plants. *Proc. Natl. Acad. Sci. USA.* **107:** 17833–17838.
78. Nakayama, M., H. Sato, T. Okuda, N. Fujisawa, N. Kono, H. Arai, E. Suzuki, M. Umeda, H. O. Ishikawa, and K. Matsuno. 2011. Drosophila carrying pex3 or pex16 mutations are models of Zellweger syndrome that reflect its symptoms associated with the absence of peroxisomes. *PLoS One.* **6:** e22984.
79. Faust, J. E., A. Verma, C. Peng, and J. A. McNew. 2012. An inventory of peroxisomal proteins and pathways in Drosophila melanogaster. *Traffic.* **13:** 1378–1392.
80. Attrill, H., K. Falls, J. L. Goodman, G. H. Millburn, G. Antonazzo, A. J. Rey, and S. J. Marygold; FlyBase Consortium. 2016. FlyBase: establishing a gene group resource for Drosophila melanogaster. *Nucleic Acids Res.* **44(D1):** D786–D792.
81. Boeszoermenyi, A., H. M. Nagy, H. Arthanari, C. J. Pillip, H. Lindermuth, R. E. Luna, G. Wagner, R. Zechner, K. Zangger, and M. Oberer. 2015. Structure of a CGI-58 motif provides the molecular basis of lipid droplet anchoring. *J. Biol. Chem.* **290:** 26361–26372.
82. Gruber, A., I. Cornaciu, A. Lass, M. Schweiger, M. Poeschl, C. Eder, M. Kumari, G. Schoiswohl, H. Wolinski, S. D. Kohlwein, et al. 2010. The N-terminal region of comparative gene identification-58 (CGI-58) is important for lipid droplet binding and activation of adipose triglyceride lipase. *J. Biol. Chem.* **285:** 12289–12298.